Construction of reduced order operators for hydroelastic vibrations of prestressed liquid–structure systems using separated parameters decomposition

Christophe Hoareau, Jean-François Deü, Roger Ohayon

Construction of reduced order operators for hydroelastic vibrations of prestressed liquid–structure systems using separated parameters decomposition[☆]

C. Hoareau[*], J.-F. Deü, R. Ohayon

Laboratoire de Mécanique des Structures et des Systèmes Couplées (LMSSC), Structural Mechanics and Coupled System Laboratory, Conservatoire national des arts et métiers (Cnam), 292 Rue Saint-Martin, 75003 Paris, France[1]

This study deals with the computation of parameterized reduced order models for hydroelastic vibrations of interior fluid–structure systems with a free surface. The main parameter is the weight of the liquid acting on the structure, which allows static and dynamic simulations for different liquid heights in a tank. Both the structure and the liquid domains are mapped in reference configurations, which constituted a first originality of the paper. The second originality of the proposed approach consists in using projections on an eigenmode basis associated with the use of an adapted SVD in order to compute the eigenfrequencies of the coupled problem. In particular, we show that the proposed approach allows to construct reduced order model involving a small number of matrices through a decomposition of linearized reduced operators in terms of separated parameters functions. Convergence analysis of numerical results is discussed showing the efficiency of the method.

Keywords: Hydroelastic vibrations; Prestressed nonlinear effects; Parameterized reduced order model; Added mass; Finite element method

1. Introduction

(i) General interior fluid–structure interaction context—This study is part of the general framework of the dynamics of structures containing free-surface liquids subjected to vibration or transient excitations. These studies are of prime importance for the aerospace industry, naval industry, nuclear industry, civil engineering and biomechanics. Efficient adapted computational methods, validated by experiments are therefore required. In addition, the methods must consider parametric variations whether for the design of the structure or for various liquid filling ratio. For example, in the aerospace industry, those parameters have huge impact on the dynamic of liquid-propelled launchers. For general problems concerning the dynamic of liquid filled structures in the aerospace domain, we refer the reader to [1,2]. Numerous semi-analytical approaches developed over the last decades have been carried out on the subject for fluid filled tanks of specific shapes such as cylinder neglecting prestresses due to liquid weight (see for instance [3–6]). Numerical studies were conducted in structural vibrations and transient dynamics, based on

[☆] A special issue in honor of the lifetime achievement of J. Tinsley Oden.

[*] Corresponding author.
E-mail address: christophe.hoareau@lecnam.net (C. Hoareau).

[1] URL: https://www.lmssc.cnam.fr/en.com.

Nomenclature

$\boldsymbol{u}$	Structural displacement vector field
$\boldsymbol{w}$	Liquid displacement vector field
$\boldsymbol{\mu}$	Vector of parameters
$\boldsymbol{u}_{\mathrm{s}}$	Static displacement vector field
p_{s}	Static pressure field
p_{d}	Dynamic pressure field
φ	Displacement potential field
Ω_{f}	Fluid domain
Ω_{s}	Solid domain
Σ_{f}	Free surface
Σ_{u}	Surface with prescribed displacements
Σ_{t}	Surface with prescribed loads
J	Jacobian determinant
Σ_{i}	Fluid–structure interface
Σ_{w}	Surface with prescribed pressure gradient
ω_{s}	Solid domain (current configuration)
ω_{f}	Fluid domain (current configuration)
γ_{i}	Fluid–structure interface (current configuration)
γ_{f}	Free surface (current configuration)
$\boldsymbol{N}$	Normal vector external to the structure
$\boldsymbol{F}$	Deformation gradient
$\boldsymbol{E}$	Green–Lagrange strain tensor
$\mathcal{D}$	Constitutive equation coefficients
$\boldsymbol{S}$	Second Piola–Kirchhoff stress tensor
ω	Circular frequency
ρ_{s}	Solid mass density
ρ_{f}	Fluid mass density
l	Liquid height
$\boldsymbol{I}$	Identity matrix
Grad	Gradient differential operator (reference coordinates)
grad	Gradient differential operator (current coordinates)
det	Determinant of a matrix
SVD	Singular value decomposition

the finite element method applied to appropriate variational formulations of the boundary value problems [7–9]. Let us also cite applications of boundary element methods for applications with fluid–structure interaction (see for instance [10]).

Due to the complexity of the systems involving prohibitive number of degrees of freedom, parametric studies needed for optimization design, control problem and experimental correlation, reduced order model have been developed in literature. For structural dynamic problems let us recall that reduced order models have been developed by projection-based method on the eigenmodes, obtained *a priori*, such as component mode methods [11,12], extended for modal fluid–structure interaction vibrations problems (see for instance [7]). For parametric studies, *a posteriori* reduced order model techniques, such as [13] for interpolation and [14,15] for projection have been carried out.

(ii) Context of the study in hydroelasticity—Concerning the liquid contained in the tank, we refer to [16], in which strong or weak coupling between physical effects such as viscosity, compressibility, free surface and internal

gravity or surface tension are discussed. When the elasticity of the tank walls is taken into account, a special and very important fluid–structure coupling situation occurs, in which effects of viscosity, compressibility, sloshing and surface tensions can be neglected with respect to the inertial effects of the fluid during the motion. The liquid will be considered here as incompressible with a free surface condition of zero fluctuation of pressure (or equivalently zero displacement potential on the free surface). This situation was initially highlighted in [17]. In the sequel, we qualify such a situation as hydroelastic vibrations involving an added mass operator (see for Refs. [7,18–20]). It is very important to underline that the effect of gravity (i.e. the liquid weight) must of course be taken into account for the calculation of the equilibrium state of the structure.

(iii) Prestressing effects—A formulation, without referring to a prestress state, but under hypotheses of weak geometric structural nonlinearities coupled with linear acoustic liquids and the surface tensions, has been presented in [21]. But here, the aim being the evaluation of the prestress effect due to liquid weight, we need to define an equilibrium prestressed state around which the linearized vibrations are calculated. Prestressing effects due to gas or liquid pressure on the hydroelastic vibrations have been analyzed using first order geometric stiffness linear operators (see Refs. [22–26]). In this paper, the prestressed state is considered as a quasi-static equilibrium state using geometric and load nonlinear models in finite strain, as done in [27,28]. In this context, it should be highlighted that the pressure exerted by liquid on the structure is a follower force due to the rotation of the outward unit normal to the current fluid–structure interface, which depends on the displacement (for general concept concerning follower forces, see [29,30]).

(iv) Novelty of the paper—In a previous paper [31], a parametric study has been investigated to evaluate the influence of the prestressed state due to liquid weight on the hydroelastic vibrations considering nonlinear geometric stiffness operators including follower forces. In addition, only the structure is mapped to a reference configuration, the liquid domain being remeshed at every parametric step. A first novelty of this paper consists in the formulation including the mapping of the liquid domain. Presently, this method is developed in the case of elastic structures of arbitrary shapes connected to a rigid part in contact with the free surface. This is the case, for example, of a rigid cylinder with flexible bottoms, for which very few experiments are available in literature (up to authors knowledge, the only study available is the Ref. [32,33]). The second novelty of this paper is the following. For each parametric value, a succession of reduced order matrices has been generated. A surrogate model of reduced matrices as a finite sum of separated parameters operators have been developed. This approximation is obtained via the use of a singular value decomposition (SVD) classically used in reduced order modeling on discretized solutions, but adapted here accordingly to the problem with small size matrices. It is shown that few operators are needed to compute the coupled hydroelastic frequencies from eigenvalues involving a short number of matrices. Numerical analyses are then presented and discussed showing the accuracy of the proposed approach.

(v) Outline—In Section 2, notations and assumptions are given. In Section 3, the structural part of the hydroelastic variational formulation is recalled from [31] for self-consistency. In Section 4, the liquid part of the coupled problem mapped in an arbitrary reference configuration is presented. In Section 5, the finite element discretized hydroelastic problem with prestressing is exposed. In Section 6, the reduced order modeling strategy is given involving projection on appropriate dry prestressed modes and a SVD of parameterized reduced matrices. In Section 7 numerical examples showing the capability of the approach and the computational low cost of the method are discussed. Finally, in Section 8 conclusion is given followed by references.

2. Fluid–structure assumptions and notations

2.1. Fluid–structure assumptions

We restrict our study to the linearized vibrations of the bottom of a tank prestressed by a liquid weight. It can be the case in aerospace applications, in particular for liquid launcher propellant tanks where the top and bottom tanks are rather flexible and light (see Fig. 1). Two particular phases are considered in the following: (**Phase1**) the filling process of the tank before launch considering that the bottom is prestressed by the liquid and (**Phase2**) the linearized hydroelastic vibrations of the bottom tank around a prestressed state at a known filling rate configuration during the flight. The problem consists in evaluating the influence of the liquid weight on the linearized vibrations as a function of the liquid height parameter and generate a parameterized reduced order model.

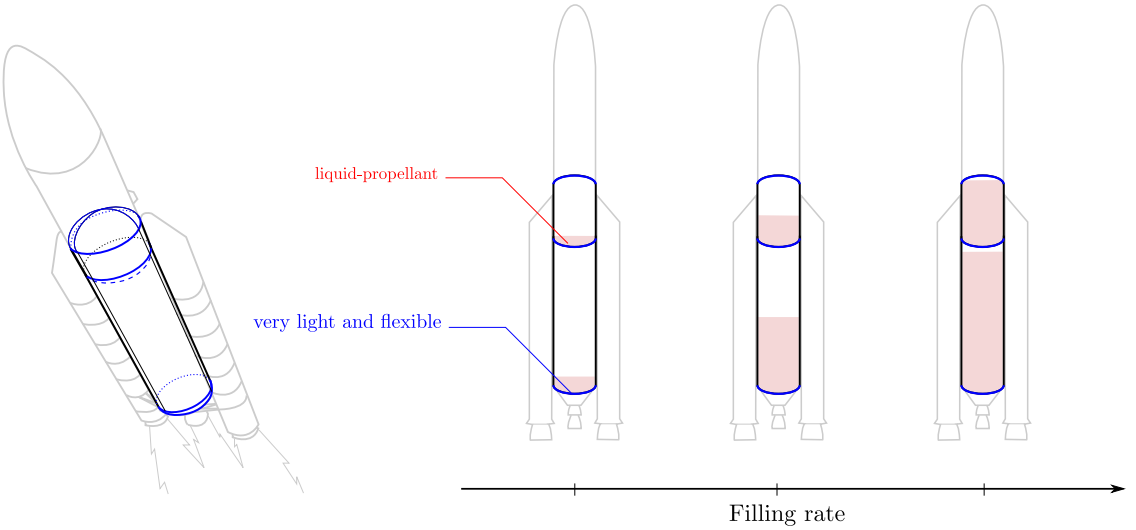

Fig. 1. Evolution of the liquid–structure system with very light and flexible parts function of a filling rate.

- **Assumptions for the solid:**
  - **Phase1**: The solid is supposed to be relevant of Saint-Venant Kirchhoff constitutive equations [34]. During the filling phase, the bottom of the tank is supposed to be prestressed due to the liquid weight. The transformation is considered to be quasi-static and the structural displacement is large enough to consider a weak nonlinear geometrical behavior of the structure.
  - **Phase2**: The solid is now prestressed. The prestressed state is due to the filling of the tank from the first phase. Thus, during the flight, the goal is to estimate the fluctuations of displacement associated with the hydroelastic natural frequencies. Those coupled vibrations analyses are dependent on parameters such as the liquid height or additional gas pressurization.
- **Assumptions for the fluid:**
  - **Phase1**: The liquid is supposed to have a horizontal free-surface under constant gravity force. The liquid is thus modeled with a hydrostatic pressure parameterized by the liquid height as seen in Fig. 2. No surface tension is considered here. The weight of the liquid is seen as a non-uniform follower force. The liquid pressure on the interface only depends on the wetted surface position.
  - **Phase2**: The fluid is supposed to be inviscid, homogeneous and incompressible. No surface tension is considered. The small amplitude motions of liquid are irrotational. Consequently, the equations of the fluid can be expressed through a scalar field namely the pressure field or the displacement potential field.

2.2. Energy considerations regarding the linearized hydroelastic vibrations

During those linearized hydroelastic vibrations, the potential energy of the free-surface of the liquid is due to gravity and the surface tension is negligible. Only the kinetic energy of the fluid and the potential and kinetic energies of the structure are considered here. The consequence is that, for the fluid dynamic equation, the free-surface condition is expressed as a zero-pressure condition (or zero-displacement potential condition). Let us recall that the gravity effect, on the fluid–structure interface, has been of course considered for the static equilibrium and in the parameterized evolution of the static prestressed states.

2.3. Notations of the fluid–structure reference domains

The fluid–structure system in its reference configuration is given in Fig. 3(a). Let Ω_s and Ω_f be open bounded domains of $\mathbb{R}^3$ which are respectively the solid and the fluid domains in their references configurations. The

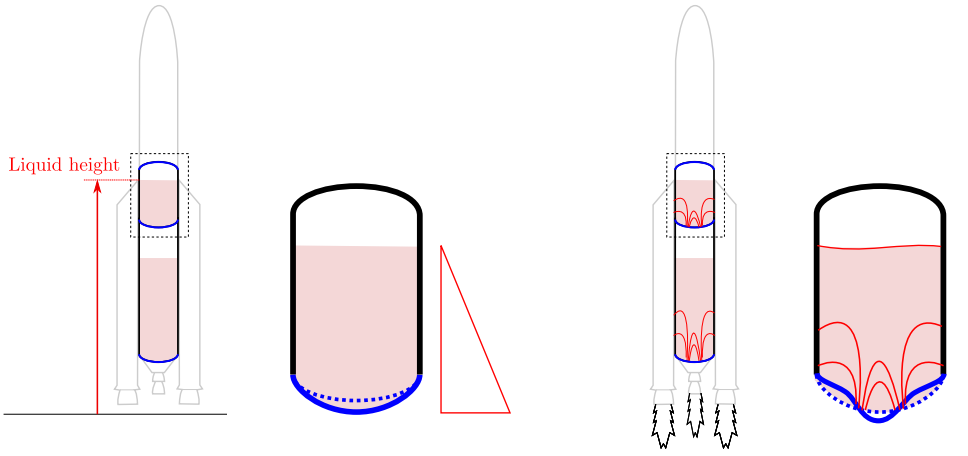

Fig. 2. (a) **Phase 1**: filling of the tank inducing a prestressing of the bottom and (b) **Phase 2**: flight with linearized hydroelastic vibrations around a prestressed state.

boundary of the solid is denoted by $\partial\Omega_s = \Sigma_u \cup \Sigma_t \cup \Sigma_i$ where Σ_u is the solid with prescribed displacements, Σ_t is a surface with prescribed dead loads, i.e. forces which are constant in magnitude and direction, and Σ_i is the fluid–structure interface. The boundary of the fluid is denoted by $\partial\Omega_f = \Sigma_i \cup \Sigma_f \cup \Sigma_w$ where Σ_f is a free-surface and Σ_w is a surface with prescribed gradient of pressure. We denote by $\boldsymbol{u} : \Omega_s \to \mathbb{R}^3$ the displacement vector field in Ω_s. We also denote by $\boldsymbol{w} : \Omega_f \to \mathbb{R}^3$ a vector field in Ω_f.

2.4. Notations of the fluid–structure parameterized current domains

In the Cartesian reference system $(O, \boldsymbol{e}_1, \boldsymbol{e}_2, \boldsymbol{e}_3)$, let $\boldsymbol{X} = (X_1, X_2, X_3)$ be the position vector of a point in the reference configuration on the solid domain and $\boldsymbol{Z} = (Z_1, Z_2, Z_3)$ be the position vector of a point in the reference configuration on the fluid domain. In a current (deformed) configuration respectively denoted by ω_s and ω_f at time t, and for a set of n parameters $\boldsymbol{\mu} = (\mu_1, \ldots, \mu_n)$, the points that are transformed from $\boldsymbol{X}$ to $\boldsymbol{x}$ and from $\boldsymbol{Z}$ to $\boldsymbol{z}$ are respectively written as:

$$\boldsymbol{x}(\boldsymbol{\mu}, \boldsymbol{X}, t) = \boldsymbol{X} + \boldsymbol{u}(\boldsymbol{\mu}, \boldsymbol{X}, t) \tag{1}$$

$$\boldsymbol{z}(\boldsymbol{\mu}, \boldsymbol{Z}, t) = \boldsymbol{Z} + \boldsymbol{w}(\boldsymbol{\mu}, \boldsymbol{Z}, t) \tag{2}$$

in which $\boldsymbol{u} = (u_1, u_2, u_3)$ and $\boldsymbol{w} = (w_1, w_2, w_3)$ are vector fields defined respectively in Ω_s and Ω_f.

3. Variational linearized formulation for the structure in contact with the liquid

This section is devoted to a recall of the linearized variational formulation for the prestressed structure in the reference configuration [31]. Let us recall from [34,35] the deformation gradient denoted by $\boldsymbol{F}$ and its Jacobian denoted by J as functions of the displacement fields:

$$\boldsymbol{F}(\boldsymbol{u}) = \boldsymbol{I} + \mathbf{Grad}\,\boldsymbol{u} \tag{3}$$

$$J(\boldsymbol{u}) = \det \boldsymbol{F}(\boldsymbol{u}) \tag{4}$$

Let $\mathcal{C}_u$ be the admissible spaces of regular displacements field defined as follows:

$$\mathcal{C}_u = \{\boldsymbol{u} \quad \text{regular}, \quad \text{such that } \boldsymbol{u} = \boldsymbol{0} \quad \text{on} \quad \Sigma_u\} \tag{5}$$

We consider here the two sub-problems, one for the filling phase and the other one for the coupled fluid–structure vibrations around the prestressed state. The prestressed state is the configuration resulting from a nonlinear static

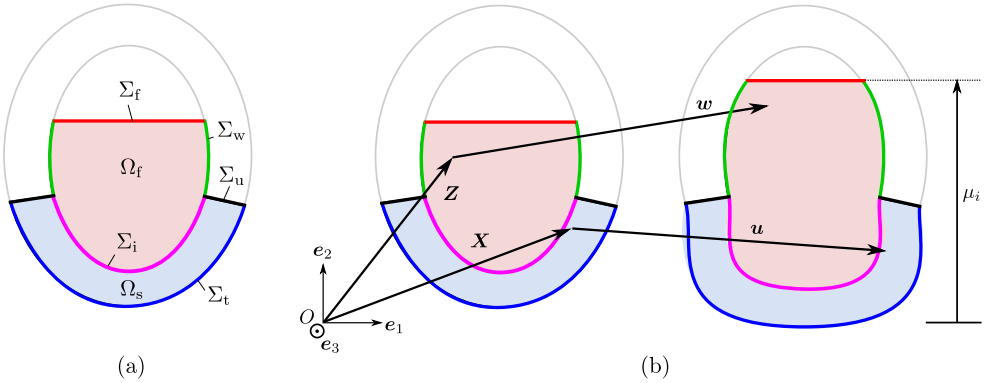

Fig. 3. (a) Reference configurations of the liquid and the structure and (b) mapping of the fluid structure domains as function of a liquid height parameter.

problem. The static displacement solution $\boldsymbol{u}_\mathrm{s}$ depends on a set of parameters denoted by $\boldsymbol{\mu}$. Knowing $\boldsymbol{u}_\mathrm{s}$, the vibration analysis problem consists in finding the dynamic fluctuation of displacement denoted by $\boldsymbol{u}_\mathrm{d}$. Then, the total displacement is expressed as follows:

$$\boldsymbol{u}(\boldsymbol{\mu}, \boldsymbol{X}, t) = \underbrace{\boldsymbol{u}_\mathrm{s}(\boldsymbol{\mu}, \boldsymbol{X})}_{\text{nonlinear static}} + \underbrace{\boldsymbol{u}_\mathrm{d}(\boldsymbol{\mu}, \boldsymbol{X}, t)}_{\text{linearized dynamic}} \tag{6}$$

The pressure in the liquid is also expressed as a sum of a static pressure p_s and a fluctuation of pressure p_d such that:

$$p(\boldsymbol{\mu}, \boldsymbol{u}_\mathrm{s}, \boldsymbol{X}, t) = p_\mathrm{s}(\boldsymbol{\mu}, \boldsymbol{u}_\mathrm{s}, \boldsymbol{X}) + p_\mathrm{d}(\boldsymbol{\mu}, \boldsymbol{X}, t) \tag{7}$$

Under those assumptions, knowing the static solution $\boldsymbol{u}_\mathrm{s}$, the dynamic part of the virtual work principle, can be written as follows:

$$k_\mathrm{t}(\boldsymbol{u}_\mathrm{s}; \boldsymbol{u}_\mathrm{d}, \delta\boldsymbol{u}) - c(\boldsymbol{u}_\mathrm{s}; p_\mathrm{d}, \delta\boldsymbol{u}) + m(\ddot{\boldsymbol{u}}_\mathrm{d}, \delta\boldsymbol{u}) = f(\delta\boldsymbol{u}) \quad \forall\, \delta\boldsymbol{u} \in \mathcal{C}_\mathrm{u} \tag{8}$$

in which $f(\delta\boldsymbol{u})$ denotes the virtual work of external forces and where k_t is the sum of the material and geometrical stiffness contribution to the internal virtual work, respectively denoted by k_m and k_g and defined as follows:

$$k_\mathrm{m}(\boldsymbol{u}_\mathrm{s}; \boldsymbol{u}_\mathrm{d}, \delta\boldsymbol{u}) = \int_{\Omega_\mathrm{s}} \delta\boldsymbol{E}(\boldsymbol{u}_\mathrm{s}, \delta\boldsymbol{u}) : \mathcal{D} : [\boldsymbol{\varepsilon}(\boldsymbol{u}_\mathrm{d}) + \boldsymbol{\gamma}(\boldsymbol{u}_\mathrm{s}, \boldsymbol{u}_\mathrm{d})]\, d\Omega \tag{9}$$

$$k_\mathrm{g}(\boldsymbol{u}_\mathrm{s}; \boldsymbol{u}_\mathrm{d}, \delta\boldsymbol{u}) = \int_{\Omega_\mathrm{s}} \boldsymbol{\gamma}(\boldsymbol{u}_\mathrm{d}, \delta\boldsymbol{u}) : \boldsymbol{S}(\boldsymbol{u}_\mathrm{s})\, d\Omega \tag{10}$$

where $\boldsymbol{S}$ is the second Piola–Kirchhoff stress tensor, $\mathcal{D}$ is the fourth order tensor of the Saint-Venant Kirchhoff constitutive equation, $\delta\boldsymbol{E}$ is the virtual expression of the Green–Lagrange strain tensor $\boldsymbol{E}$ defined as follows:

$$\boldsymbol{E}(\boldsymbol{u}_\mathrm{s}) = \frac{1}{2}(\boldsymbol{F}^\mathrm{T}(\boldsymbol{u}_\mathrm{s})\boldsymbol{F}(\boldsymbol{u}_\mathrm{s}) - \boldsymbol{I}) \tag{11}$$

and $\boldsymbol{\varepsilon}$ and $\boldsymbol{\gamma}$ are respectively the linear and the linearized quadratic parts of the Green–Lagrange strain tensor, such that for two displacement fields denoted by $\boldsymbol{u}$ and $\boldsymbol{v}$, the operators are defined as follows:

$$\boldsymbol{\varepsilon}(\boldsymbol{u}) = \frac{1}{2}[\mathbf{Grad}^\mathrm{T}\boldsymbol{u} + \mathbf{Grad}\,\boldsymbol{u}] \tag{12}$$

$$\boldsymbol{\gamma}(\boldsymbol{u}, \boldsymbol{v}) = \frac{1}{2}[\mathbf{Grad}^\mathrm{T}\boldsymbol{u}\mathbf{Grad}\,\boldsymbol{v} + \mathbf{Grad}^\mathrm{T}\boldsymbol{v}\,\mathbf{Grad}\,\boldsymbol{u}] \tag{13}$$

The virtual mass operator is given by:

$$m(\ddot{\boldsymbol{u}}, \delta\boldsymbol{u}) = \rho_\mathrm{s} \int_{\Omega_\mathrm{s}} \ddot{\boldsymbol{u}} \cdot \delta\boldsymbol{u}\, dV \tag{14}$$

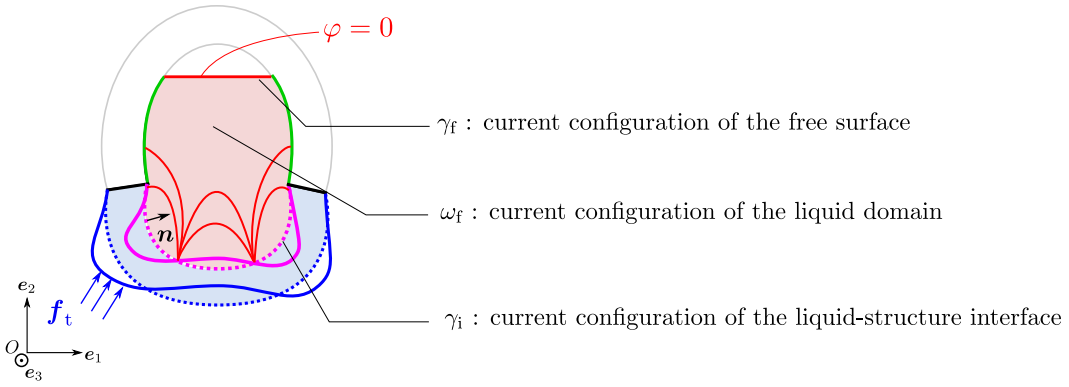

Fig. 4. Linearized hydroelastic vibrations around a prestressed state.

and the virtual structure–liquid coupling term between p_d and $\delta \boldsymbol{u}$ is defined as follows:

$$c(\boldsymbol{u}_s;\, p_d,\, \delta \boldsymbol{u}) = -\int_{\Sigma_i} p_d J(\boldsymbol{u}_s) \boldsymbol{F}^{-T}(\boldsymbol{u}_s) \boldsymbol{N} \cdot \delta \boldsymbol{u}\, dS \tag{15}$$

The terms p_d and $\boldsymbol{u}_d$ are unknown and coupled on Σ_i. The equations in the liquid will be detailed in Section 4 with a change of variable of the pressure in terms of the displacement potential. It can be noted that the internal and external works associated to the static part are both cubic forms of the unknown displacement $\boldsymbol{u}_s$.

The dynamic problem around the prestressed state modeled in Eq. (8) corresponds to a situation where the static configuration is supposed to be known. Thus, the static solution $\boldsymbol{u}_s$ must be determined before any vibrations analysis. The prestressing is involved through the contribution of geometric and material stiffness in $k_t(\boldsymbol{u}_s;\, \boldsymbol{u}_d,\, \delta \boldsymbol{u})$.

4. Variational formulation for the liquid mapped in a reference configuration

The following section is devoted to the formulation of the linearized harmonic equations in terms of the displacement potential field. We recall that in Eq. (8) two unknowns are involved: dynamic structural displacement field $\boldsymbol{u}_d$ and the dynamic liquid pressure field p_d. The later will be expressed in terms of the displacement potential field denoted by φ.

4.1. Local liquid equations in terms of the displacement potential

As we consider here the linearized vibrations of the liquid–structure system (see Fig. 4), the motions of the inviscid liquid are irrotational [16]. Consequently, the dynamic displacement field of liquid denoted by $\boldsymbol{w}_d$ is derived from a potential displacement φ, defined up to an additive constant, with respect to the current liquid configuration. The dynamic pressure p_d and the liquid displacement field $\boldsymbol{w}_d$ are given as follows:

$$w_d = \mathbf{grad}\varphi \quad \text{in} \quad \omega_f \tag{16}$$

$$p_d = -\rho \ddot{\varphi} \quad \text{in} \quad \omega_f \tag{17}$$

The liquid equations are then written in terms φ as follows:

$$\left\{ \begin{array}{lll} \Delta\varphi & = 0 & \text{in } \omega_f \quad \text{(a)} \\ \mathbf{grad}\varphi \cdot \boldsymbol{n} & = \boldsymbol{u}_d \cdot \boldsymbol{n} & \text{in } \gamma_i \quad \text{(b)} \\ \varphi & = 0 & \text{in } \gamma_f \quad \text{(c)} \end{array} \right. \tag{18}$$

- Eq. (18) corresponds to the incompressibility condition.
- Eq. (18) corresponds to the normal displacement continuity between the normal fluid displacement field $\boldsymbol{w}_d \cdot \boldsymbol{n}$ and the normal solid displacement field $\boldsymbol{u}_d \cdot \boldsymbol{n}$ on the liquid–structure interface denoted by $\boldsymbol{\gamma}_i$, in which $\boldsymbol{n}$ denotes the external unit normal with respect to the solid on its current configuration.

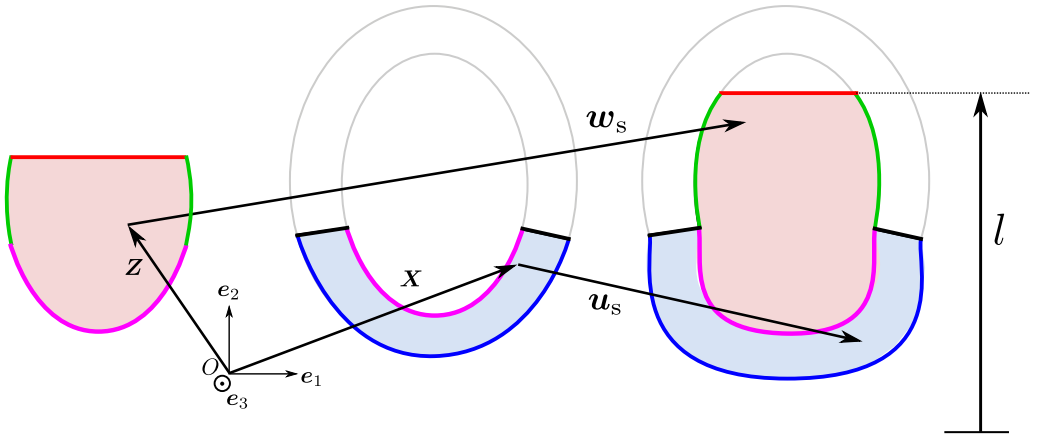

Fig. 5. Liquid domain deformation with a conformal mapping parameterized by liquid height l.

- Eq. (18) corresponds to zero potential condition on the free-surface γ_{f} which ensures the uniqueness of φ. Furthermore, it is in coherence with the hydroelastic condition related to the zero-pressure on the free-surface discussed in the energy consideration in Section 2:

$$p_{\mathrm{d}} = 0 \quad \text{in} \quad \gamma_{\mathrm{f}} \tag{19}$$

4.2. Mapping of the reference liquid domain on a current liquid configuration

The formulation associated to the linearized hydroelastic vibrations necessitates the definition of the domain liquid domain mapping, the static liquid domain displacement, denoted as $\boldsymbol{w}_{\mathrm{s}}(l, \boldsymbol{Z})$ from a chosen reference configuration Ω_{f} on its current (static) configuration ω_{f} such that:

$$\boldsymbol{w}(l, \boldsymbol{Z}, t) = \underbrace{\boldsymbol{w}_{\mathrm{s}}(l, \boldsymbol{Z})}_{\text{static liquid domain displacement field}} + \underbrace{\boldsymbol{w}_{\mathrm{d}}(l, \boldsymbol{Z}, t)}_{\text{dynamic liquid displacement field}} \tag{20}$$

where $\boldsymbol{w}_{\mathrm{d}}$ is the fluctuation of displacement field, around the configuration at rest. The parameter l is the liquid height as seen in Fig. 5. Ways to obtain $\boldsymbol{w}_{\mathrm{s}}$ consist in solving for examples a Laplacian vector equation or a fictitious linear or nonlinear elastic model or a bi-harmonic equation (see for instance [36]).

4.3. Weak variational formulation of the liquid equation in the reference configuration

The variational formulation of Eqs. (18) in the current configuration of the fluid is written as:

$$\int_{\omega_{\mathrm{f}}} \mathbf{grad}\varphi \cdot \mathbf{grad}\delta\varphi \, dv + \int_{\gamma_{\mathrm{i}}} \boldsymbol{u}_{\mathrm{d}} \cdot \boldsymbol{n} \, \delta\varphi \, ds = 0 \quad \forall \delta\varphi \in \mathcal{C}_{\varphi} \tag{21}$$

where $\mathcal{C}_{\varphi}$ the space of regular functions defined on ω_{f} and verifying Eq. (18). The integrals in Eq. (21) can be written through the reciprocal mapping, in the reference configuration, defined in Section 3, such that:

$$\int_{\omega_{\mathrm{f}}} \mathbf{grad}\varphi \cdot \mathbf{grad}\delta\varphi \, dv = \int_{\Omega_{\mathrm{f}}} \mathbf{Grad}^{\mathrm{T}}\varphi \boldsymbol{F}^{-\mathrm{T}}(\boldsymbol{w}_{\mathrm{s}}) \cdot \boldsymbol{F}^{-1}(\boldsymbol{w}_{\mathrm{s}}) \mathbf{Grad}\, \delta\varphi \, J(\boldsymbol{w}_{\mathrm{s}}) \, dV \tag{22}$$

$$\int_{\gamma_{\mathrm{i}}} \delta\varphi \boldsymbol{n} \cdot \boldsymbol{u}_{\mathrm{d}} \, ds = \int_{\Sigma_{\mathrm{i}}} \delta\varphi \, J(\boldsymbol{w}_{\mathrm{s}}) \boldsymbol{F}^{-\mathrm{T}}(\boldsymbol{w}_{\mathrm{s}}) \boldsymbol{N} \cdot \boldsymbol{u}_{\mathrm{d}} \, dS \tag{23}$$

For sake of brevity, the same notations for the unknown fields $\boldsymbol{u}_{\mathrm{d}}$ and φ are used either in the current configurations and the reference configuration. Finally, the problem expressed in terms of the variable φ (instead of p_{d}) and $\boldsymbol{u}_{\mathrm{d}}$, can be written as follows:

$$h(\boldsymbol{w}_{\mathrm{s}}; \delta\varphi, \varphi) - c(\boldsymbol{w}_{\mathrm{s}}; \delta\varphi, \boldsymbol{u}_{\mathrm{d}}) = 0, \quad \forall \delta\varphi \in \mathcal{C}_{\varphi} \tag{24}$$

where the operator h corresponds to the virtual work of the fluid kinetic energy and the operator c, already defined in Eq. (15), corresponds to the liquid–structure coupling between $\delta\varphi$ and $\boldsymbol{u}_{\mathrm{d}}$ given as follows:

$$h(\boldsymbol{w}_{\mathrm{S}};\varphi,\delta\varphi)=\int_{\Omega_{\mathrm{f}}}\mathbf{Grad}^{\mathrm{T}}\varphi\boldsymbol{F}^{-T}(\boldsymbol{w}_{\mathrm{s}})\boldsymbol{F}^{-1}(\boldsymbol{w}_{\mathrm{s}})\mathbf{Grad}\delta\varphi\,J(\boldsymbol{w}_{\mathrm{s}})\,dV \tag{25}$$

$$c(\boldsymbol{w}_{\mathrm{s}};\delta\varphi,\boldsymbol{u}_{\mathrm{d}})=-\int_{\Sigma_{\mathrm{i}}}\delta\varphi\,J(\boldsymbol{w}_{\mathrm{s}})\boldsymbol{F}^{-\mathrm{T}}(\boldsymbol{w}_{\mathrm{s}})\boldsymbol{N}\cdot\boldsymbol{u}_{\mathrm{d}}\,dS \tag{26}$$

The term $\boldsymbol{F}^{-1}(\boldsymbol{w}_{\mathrm{s}}(l))$ involved in Eq. (25) depends on the liquid height parameter l.

Finally, Eqs. (8) and (24) and appropriate initial conditions correspond to the weak variational formulation of the prestressed hydroelastic problem.

5. Prestressed hydroelastic vibration problem and finite element discretization

5.1. Continuous formulation of the prestressed hydroelastic vibration problem

We consider the linearized vibrations of the fluid–structure system around a known equilibrium state (defined as the prestressed state which depends on the fluid height) as seen in Fig. 4. Then we have:

$$\boldsymbol{u}_{\mathrm{d}}(\boldsymbol{X},t,\omega)=\boldsymbol{u}_{\mathrm{d}}(\boldsymbol{X})\exp(j\omega t)\quad\text{and}\quad\delta\boldsymbol{u}(\boldsymbol{X},t,\omega)=\delta\boldsymbol{u}(\boldsymbol{X})\exp(j\omega t) \tag{27}$$

$$\varphi(\boldsymbol{Z},t,\omega)=\varphi(\boldsymbol{Z})\exp(j\omega t)\quad\text{and}\quad\delta\varphi(\boldsymbol{Z},t,\omega)=\delta\varphi(\boldsymbol{Z})\exp(j\omega t) \tag{28}$$

We have kept the same notation for $\boldsymbol{u}_{\mathrm{d}}(\boldsymbol{X},t,\omega)$ and $\boldsymbol{u}_{\mathrm{d}}(\boldsymbol{X})$ for sake of simplicity ($\boldsymbol{u}_{\mathrm{d}}(\boldsymbol{X})$ represents the maximum amplitude of $\boldsymbol{u}_{\mathrm{d}}$ during time t). The same abuse of notation applies for φ, $\delta\boldsymbol{u}$ and $\delta\varphi$. Consequently, the acceleration of the dynamic displacement is the following:

$$\ddot{\boldsymbol{u}}_{\mathrm{d}}=-\omega^2\boldsymbol{u}_{\mathrm{d}} \tag{29}$$

Knowing $\boldsymbol{u}_{\mathrm{s}}$ and $\boldsymbol{w}_{\mathrm{s}}$, the linearized harmonic problem consists in finding $\boldsymbol{u}\in\mathcal{C}_{\mathrm{u}}$ and $\Phi\in\mathcal{C}_{\varphi}$ such that:

$$k_{\mathrm{t}}(\boldsymbol{u}_{\mathrm{s}};\boldsymbol{u}_{\mathrm{d}},\delta\boldsymbol{u})-\omega^2m(\boldsymbol{u}_{\mathrm{d}},\delta\boldsymbol{u})-\omega^2\rho_{\mathrm{f}}c(\boldsymbol{u}_{\mathrm{s}};\varphi,\delta\boldsymbol{u})=f(\delta\boldsymbol{u}),\qquad\forall\,\delta\boldsymbol{u}\;\in\;\mathcal{C}_{\mathrm{u}} \tag{30}$$

$$h(\boldsymbol{w}_{\mathrm{s}};\delta\varphi,\varphi)-c(\boldsymbol{w}_{\mathrm{s}};\delta\varphi,\boldsymbol{u}_{\mathrm{d}})=0,\qquad\forall\delta\varphi\;\in\;\mathcal{C}_{\varphi} \tag{31}$$

When neglecting prestress effects, the corresponding $(\boldsymbol{u}_{\mathrm{d}},\varphi)$ formulation is classic and can be found for example in [7], chapter 5.

5.2. Finite element discretization of the prestressed parameterized hydroelastic problem

We consider a finite element discretization of the structural domain denoted by $\Omega_{\mathrm{s}}^{\mathrm{h}}$ and the liquid domain denoted by $\Omega_{\mathrm{f}}^{\mathrm{h}}$. The two meshes are supposed to be compatible at the fluid–structure interface $\Sigma_{\mathrm{i}}^{\mathrm{h}}$. We define as follows $\boldsymbol{u}_{\mathrm{d}}^{\mathrm{h}}$ and φ^{h} such that:

$$\boldsymbol{u}_{\mathrm{d}}^{\mathrm{h}}=\mathbf{N}_{\mathrm{u}}\mathbf{U}_{\mathrm{d}}\quad\text{and}\quad\varphi^{\mathrm{h}}=\mathbf{N}_{\varphi}\boldsymbol{\Phi} \tag{32}$$

$$\delta\boldsymbol{u}^{\mathrm{h}}=\mathbf{N}_{\mathrm{u}}\delta\mathbf{U}\quad\text{and}\quad\delta\varphi^{\mathrm{h}}=\mathbf{N}_{\varphi}\delta\boldsymbol{\Phi} \tag{33}$$

where $\mathbf{U}_{\mathrm{d}}$ corresponds to the unknown nodal vector amplitude of the dynamic displacements fields in the structural domain and $\boldsymbol{\Phi}$ the unknown nodal vector of the amplitude of potential of displacement field in the liquid domain. The discretized hydroelastic problem coupling displacement field $\mathbf{U}_{\mathrm{d}}$ and displacement potential field $\boldsymbol{\Phi}$ is then reduced to an eigenvalue problem written as follows:

$$\left(\begin{bmatrix}\mathbf{K}_{\mathrm{t}}(\boldsymbol{\mu},\boldsymbol{u}_{\mathrm{s}}^{\mathrm{h}}) & \mathbf{O}\\ \mathbf{O} & \mathbf{O}\end{bmatrix}-\omega^2\begin{bmatrix}\mathbf{M} & \rho_{\mathrm{f}}\mathbf{C}(\boldsymbol{u}_{\mathrm{s}}^{\mathrm{h}})\\ \rho_{\mathrm{f}}\mathbf{C}^{\mathrm{T}}(\boldsymbol{w}_{\mathrm{s}}^{\mathrm{h}}) & -\rho_{\mathrm{f}}\mathbf{H}(\boldsymbol{\mu},\boldsymbol{w}_{\mathrm{s}}^{\mathrm{h}})\end{bmatrix}\right)\begin{pmatrix}\mathbf{U}_{\mathrm{d}}\\ \boldsymbol{\Phi}\end{pmatrix}=\begin{pmatrix}\mathbf{0}\\ \mathbf{0}\end{pmatrix} \tag{34}$$

where all the operators are defined such that:

$$k_{\mathrm{t}}(\boldsymbol{u}_{\mathrm{s}}^{\mathrm{h}};\boldsymbol{u}_{\mathrm{d}}^{\mathrm{h}},\delta\boldsymbol{u}^{\mathrm{h}})=\delta\mathbf{U}^{\mathrm{T}}\mathbf{K}_{\mathrm{t}}\mathbf{U}_{\mathrm{d}} \tag{35}$$

$$c(\boldsymbol{u}_{\mathrm{s}}^{\mathrm{h}};\varphi^{\mathrm{h}},\delta\boldsymbol{u}^{\mathrm{h}})=\delta\mathbf{U}^{\mathrm{T}}\mathbf{C}\boldsymbol{\Phi} \tag{36}$$

$$m(\boldsymbol{u}_{\mathrm{d}}^{\mathrm{h}},\delta\boldsymbol{u}^{\mathrm{h}})=\delta\mathbf{U}^{\mathrm{T}}\mathbf{M}\mathbf{U}_{\mathrm{d}} \tag{37}$$

$$h(\boldsymbol{w}_{\mathrm{s}}^{\mathrm{h}};\delta\varphi^{\mathrm{h}},\varphi^{\mathrm{h}}) = \delta\boldsymbol{\Phi}^{\mathrm{T}}\mathbf{H}\boldsymbol{\Phi} \tag{38}$$

$$c(\boldsymbol{w}_{\mathrm{s}}^{\mathrm{h}};\delta\varphi^{\mathrm{h}},\boldsymbol{u}_{\mathrm{d}}^{\mathrm{h}}) = \delta\boldsymbol{\Phi}^{\mathrm{T}}\mathbf{C}^{\mathrm{T}}\mathbf{U}_{\mathrm{d}} \tag{39}$$

where $\mathbf{K}_{\mathrm{t}}$ the tangent matrix of the structure around a prestressed state, $\mathbf{M}$ the mass matrix, $\mathbf{C}$ corresponds to a coupling matrix at the fluid–structure interface and $\mathbf{H}$ is the matrix of potential of displacement gradient. Due to the zero-potential displacement condition on the free surface, the associated sub-matrices are denoted by $\mathbf{H}^*$, $\mathbf{C}^*$ and $\mathbf{C}^{*\mathrm{T}}$. The matrix $\mathbf{H}^*$ is invertible (we recall that the dimension of the kernel of $\mathbf{H}^*$ is one). Thus, we can write:

$$[\mathbf{K}_{\mathrm{t}} - \omega^2(\mathbf{M}+\mathbf{M}_{\mathrm{a}})]\mathbf{U}_{\mathrm{d}} = \mathbf{0} \quad \text{with} \quad \mathbf{M}_{\mathrm{a}} = \rho_{\mathrm{f}}\mathbf{C}^*(\mathbf{H}^*)^{-1}\mathbf{C}^{*\mathrm{T}} \tag{40}$$

$$\mathbf{H}^*\boldsymbol{\Phi}^* = \mathbf{C}^{*\mathrm{T}}\mathbf{U}_{\mathrm{d}} \tag{41}$$

where $\mathbf{M}_{\mathrm{a}}$ is the added mass matrix (symmetric, positive-definite). We obtain the eigenmodes of Eq. (40) completed by Eq. (41):

$$\left\{\omega_\alpha^2, \begin{pmatrix}\mathbf{U}_\alpha \\ \boldsymbol{\Phi}_\alpha\end{pmatrix}\right\}_{\alpha=1\ldots n_{\mathrm{h}}} \tag{42}$$

where n_{h} is the number of desired hydroelastic modes. The modal pressure $\mathbf{P}_\alpha$ is then obtained as:

$$\mathbf{P}_\alpha = \rho_{\mathrm{f}}\omega_\alpha^2\boldsymbol{\Phi}_\alpha \tag{43}$$

The evaluation of the eigenmodes of the coupled system must be performed for each set of loading parameters, which can become expensive in terms of computational time, especially for matrices with a lack of sparsity [37]. Therefore, it is relevant to use modal-based projection approaches to accelerate the evaluation of eigenfrequencies for parametric studies.

6. Methodology of model order reduction

6.1. Projection based reduced order model: projection on dry modes

The computation of the hydroelastic eigenfrequencies can be done considering the solution of an eigenvalue problem requiring the construction of an added mass matrix. This matrix involves only the structural degrees of freedom on the liquid–structure interface but is a full on the lines and columns which is a drawback from numerical point of view. The computation of $\mathbf{M}_{\mathrm{a}}$ being costly, several specific methods have been developed in the literature (see for instance [38] for Schur complement computation and [37]). Here the matrices $\mathbf{K}_{\mathrm{t}}$ and $\mathbf{H}$ change with respect to the liquid height. Therefore, it is proposed in this paper an alternative procedure based on projection on a "parametric prestressed dry" basis dependent on the liquid height l.

The main idea is based on a preliminary calculation of the modes of the structure without the added mass operator. Fig. 6(a) represents the evolution of the first 5 coupled frequencies as a function of the liquid height parameter l. The approach described in Fig. 6(b) can be decomposed into 5 steps, for a given value of l_i:

- **S1**: Construction of an eigenvalue problem around a prestressed state knowing the tangent matrix $\mathbf{K}_{\mathrm{t}}(l_i)$ and the mass matrix $\mathbf{M}$.
- **S2**: Generation of the matrix $\mathbf{B}_{\mathrm{u}}$ with the n_{dry} first vectors basis $\mathbf{u}_\beta$ associated with increasing circular frequencies ω_β.
- **S3**: Solving n_{dry} linear systems using $\mathbf{H}$ and the transpose of the coupling matrix $\mathbf{C}^{\mathrm{T}}$, for each appropriate prestressed dry mode $\mathbf{u}_\beta$. The fluid responses $\boldsymbol{\Phi}_\beta$ are stored in a matrix $\mathbf{B}_\varphi$.
- **S4**: Construction of the reduced operators $\mathbf{K}_{\mathrm{r}}$, $\mathbf{M}_{\mathrm{r}}$ and $\mathbf{M}_{\mathrm{ar}}$. These operators are of size $(n_{\mathrm{dry}} \times n_{\mathrm{dry}})$.
- **S5**: Solving the reduced eigenvalue problem with reduced added mass matrix:

$$[\mathbf{K}_{\mathrm{r}} - \omega^2(\mathbf{M}_{\mathrm{r}}+\mathbf{M}_{\mathrm{ar}})]\boldsymbol{\kappa} = \mathbf{0} \tag{44}$$

The eigenvalues of this system give us the frequencies of hydroelastic resonances (as shown in Fig. 6(a)).

This methodology has the advantage of allowing the calculation of a reduced added mass operator without the construction of a full operator at the interface. It is nevertheless dependent on the number of prestressed dry modes that have to be chosen beforehand. To our knowledge, no method allows to determine the optimal number of selected dry modes. This approach has been used in [31] and has shown a good comparison with experimental results from [32].

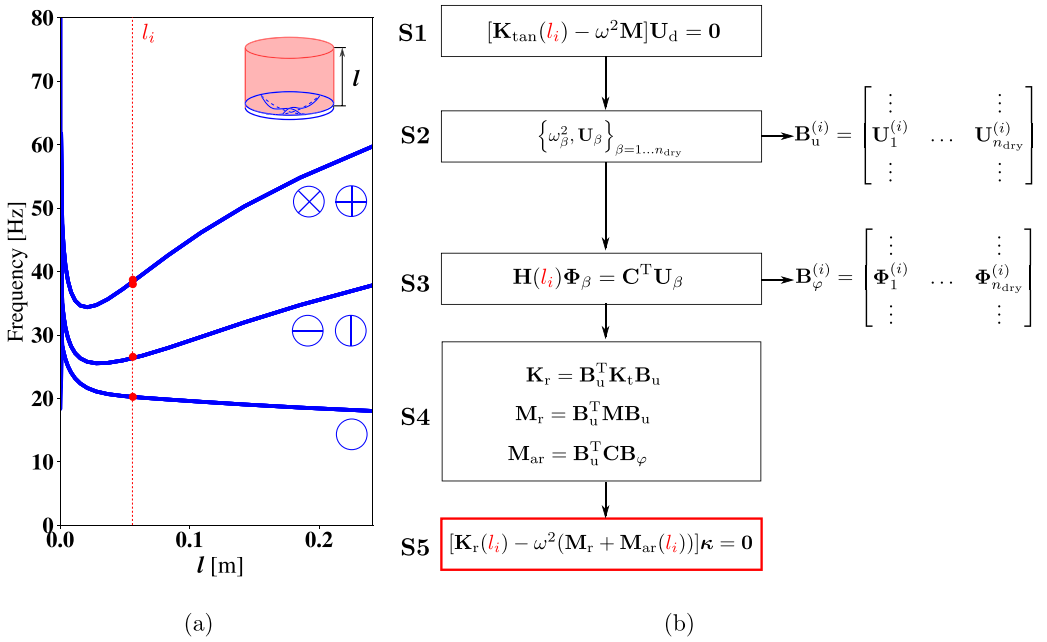

Fig. 6. (a) Evolution of hydroelastic eigenfrequencies of a circular plate bottom with prestressing function of liquid height (see for instance [32] for experimental reference values); (b) Methodology for the calculation of hydroelastic eigenvalues by projection on parametric prestressed dry basis ($n_\mathrm{dry} = 10$ for this example).

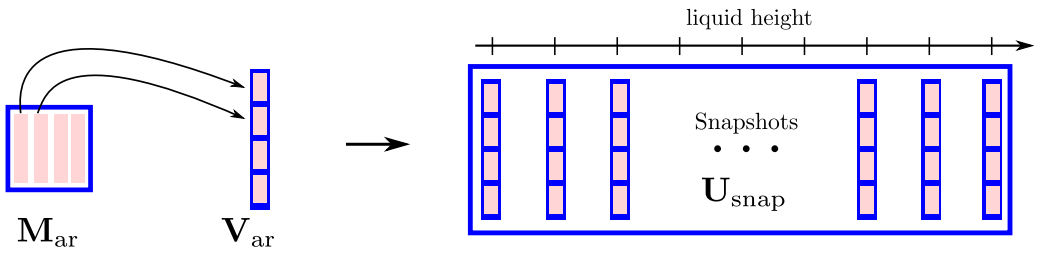

Fig. 7. Construction of a snapshot matrix from the reduced added mass matrices.

6.2. Separated variables reduced operators and surrogate models

The Eq. (44) requires the construction of reduced operators $\mathbf{K}_\mathrm{r}$ and $\mathbf{M}_\mathrm{ar}$ for each value of the parameter l_i. This section is devoted to the approximation of these operators as linear combinations of reduced operators.

6.2.1. Reduced matrices as finite sum of reduced operators

The matrices $\mathbf{M}_\mathrm{ar}$ and $\mathbf{K}_\mathrm{r}$ depend on the number of selected dry modes n_dry selected modes. The size of the matrices are assumed to be small compared to the number of degrees of freedom of the full problem. The methodology is detailed as follows: for a given reduced added mass matrix $\mathbf{M}_\mathrm{ar}$, an associated vector $\mathbf{V}_\mathrm{ar}$ containing all the columns of the reduced matrix is generated as shown in Fig. 7. This methodology is also applied to the reduced stiffness matrix. Each vector can be concatenated into a snapshot matrix $\mathbf{U}_\mathrm{snap}$. From the snapshot matrix, a singular value decomposition (SVD) is performed to extract the matrices $\mathbf{U}$, $\boldsymbol{\Sigma}$ et $\mathbf{V}$:

$$\mathbf{U}_\mathrm{snap} = \mathbf{U}\boldsymbol{\Sigma}\mathbf{V}^\mathrm{T} \tag{45}$$

The first vectors of the $\mathbf{U}$ matrix contain the numerical information needed to reconstruct the matrices as illustrated in Fig. 8. The first rows of the matrix $\boldsymbol{\Sigma}\mathbf{V}^\mathrm{T}$ correspond to the contributions of each matrix according to the parameter.

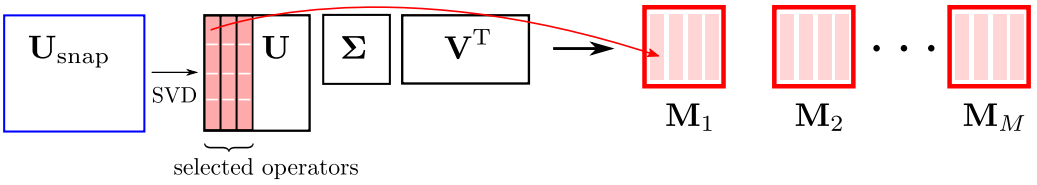

Fig. 8. Generation of reduced matrices from a SVD.

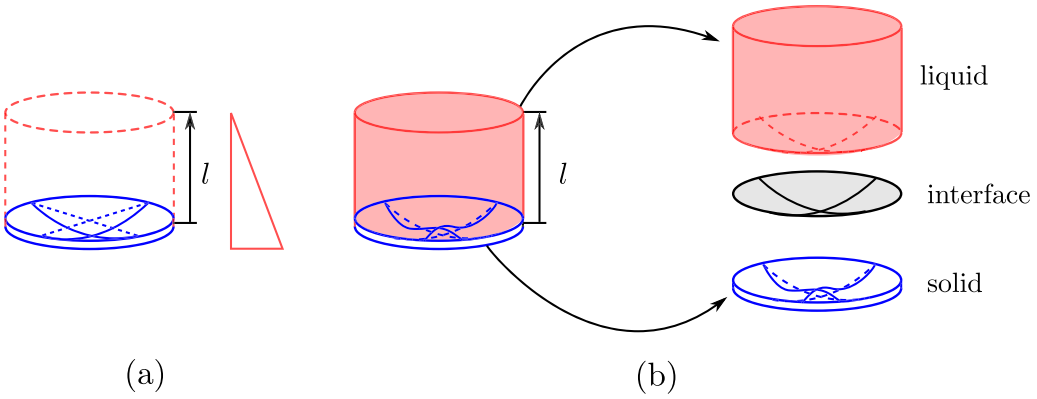

Fig. 9. (a) Prestressed state of the flexible bottom as a function of the liquid height l and (b) liquid–structure domains and interface.

Thus, this methodology allows us to generate matrices to reconstruct an approximation of $\mathbf{M}_{\text{ar}}$ and $\mathbf{K}_{\text{r}}$ through linear combinations as follows:

$$\mathbf{M}_{\text{ar}} \simeq \sum_{i=1}^{M} \theta_i(l)\mathbf{M}_i \tag{46}$$

$$\mathbf{K}_{\text{r}} \simeq \sum_{i=1}^{K} \eta_i(l)\mathbf{K}_i \tag{47}$$

The coefficients $\eta_i(l)$ and $\theta_i(l)$ are currently obtained from the SVD. If the model can be written as products of functions with separate variables, $\mathbf{K}_{\text{r}}$ can be expressed as a finite sum of computed matrices *a priori*. This situation is out of scope of this article and will be the purpose of further investigations. However, to our knowledge, no expression of $\mathbf{M}_{\text{ar}}$ written in a separated form has been formulated in the literature.

7. Numerical examples

7.1. Chiba prestressed experiment [32]

Let us recall that the methodology presented previously is based on the experiment from [32] illustrated in Fig. 9.

The objective is to evaluate the linearized hydroelastic vibrations of a thin polyester sheet, of circular shape, located under a water column. The static solution of the nonlinear problem is assumed to be known. The liquid is in contact with the upper surface of the structure which is embedded on its edge. The lower surface of the disc is free of charge. The height of the liquid varies from $l_{\text{min}} = 0$ mm to $l_{\text{max}} = 250$ mm. The material parameters are the Young's modulus $E = 6.9 \times 10^9$ Pa, the Poisson's ratio $\nu = 0.38$ and the density of the solid $\rho_{\text{s}} = 1.4 \times 10^3$ kg.m^{-3}. The density of the liquid is $\rho_{\text{f}} = 1.0 \times 10^3$ kg.m^{-3}. Regarding the finite element discretization, serendipity 3D quadratic hexahedral elements have been used for both liquid and solid reference domains discretization. The number of degrees of freedom is high enough after several mesh convergence analyses on the first five eigenfrequencies.

Two case studies are presented below:

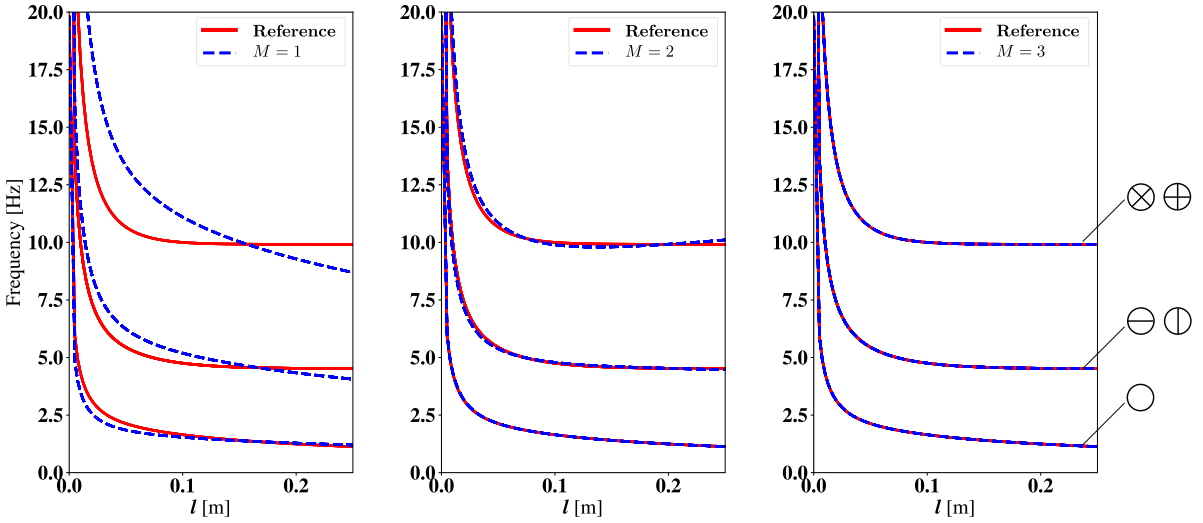

Fig. 10. Evolution of the hydroelastic eigenfrequencies as a function of the loading parameter l for three reduced added mass matrices $\mathbf{M}_{i,i=1...3}$.

- **Hydroelastic analysis of hydroelastic vibrations without prestressing**: This study highlights the added mass effect. In this configuration, the analysis of the curves shows that the added mass effect tends to decrease the frequencies as a function of l. These results also allow us to evaluate the frequencies for different numbers of reduced matrices involved in Eq. (46).
- **Hydroelastic vibrations with prestress:** The effect of prestress on the coupled hydroelastic behavior is analyzed. The added mass effect tends to decrease the frequencies as a function of l for small values of l. However, the effect of prestress tends to increase the hydroelastic frequencies (except for mode 1). We can evaluate here the number of reduced matrices $\mathbf{K}_i$, from Eq. (47), necessary to converge to the frequencies of the reference problem.

7.1.1. Hydroelastic problem with added mass and without prestressing

The eigenvalue problem below allows us to calculate the hydroelastic frequencies without pre-stressing:

$$\left[\mathbf{K}_{\mathrm{r}}^{\mathrm{lin}} - \omega^2 \left(\mathbf{M}_{\mathrm{r}} + \sum_{i=1}^{M} \theta_i(l)\mathbf{M}_i\right)\right]\boldsymbol{\kappa} = \mathbf{0} \tag{48}$$

The results in Fig. 10 show the evolution of the first 5 hydroelastic frequencies as a function of l. The red curve corresponds to the case obtained with the initial snapshots of operators and will be written "Reference" in Figs. 10 and 12 and the blue dashed curve corresponds to the reconstructed solutions. We note that few reduced matrices $\mathbf{M}_i$ are sufficient to reconstruct the resonance frequencies. We plot in Fig. 11 the first three coefficients θ_i as a function of the loading parameter. These coefficients are the contributions of the first three matrices obtained via the SVD. The first modes have larger contributions than the following modes. The fluctuations of the coefficients, function of l, are more and more important when the number of modes increases.

7.1.2. Hydroelastic problem with prestressing and added mass

The eigenvalue problem below allows us to calculate the hydroelastic frequencies with prestressing:

$$\left[\sum_{i=1}^{K} \eta_i(l)\mathbf{K}_i - \omega^2 \left(\mathbf{M}_{\mathrm{r}} + \sum_{i=1}^{M} \theta_i(l)\mathbf{M}_i\right)\right]\boldsymbol{\kappa} = \mathbf{0} \tag{49}$$

In a similar way to the previous study, Fig. 12 shows the evolution of the first 5 hydroelastic frequencies taking account prestress effect. The number of matrices $\mathbf{M}_i$ is fixed at three on all curves. Only the number of $\mathbf{K}_i$ matrices varies from one graph to another. As for the mass matrices, the number of reduced stiffness matrices

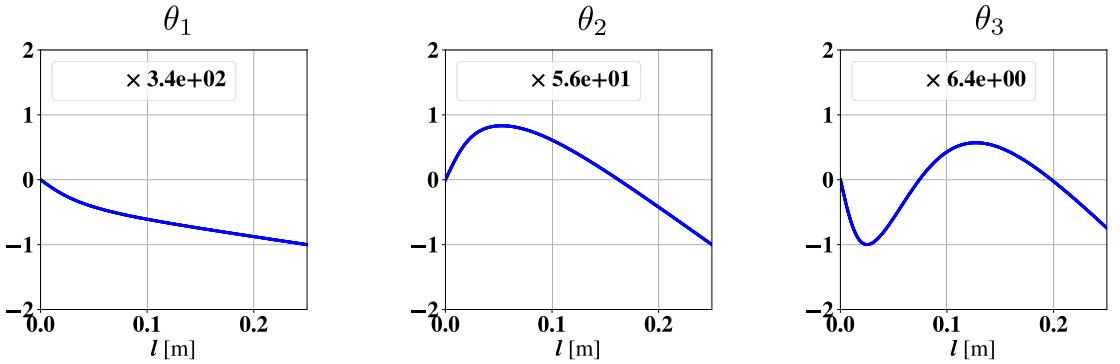

Fig. 11. Contributions of the reduced added mass matrices obtained via SVD as a function of the parameter l.

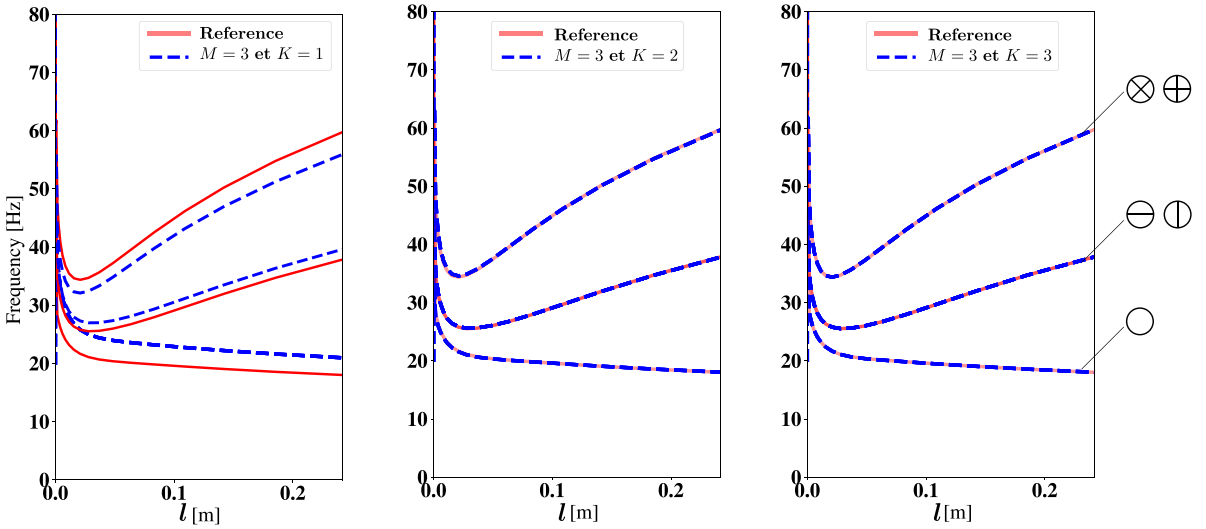

Fig. 12. Evolution of hydroelastic eigenfrequencies with prestress as a function of the loading parameter l for three reduced stiffness matrices $\mathbf{K}_{i,i=1...3}$.

$\mathbf{K}_i$ for convergence remains small in this example. We plot in Fig. 13 the first three coefficients η_i as a function of the loading parameter.

The computation time of the reduced model is here independent of the number of degrees of freedom of the reference problem. It can be solved almost in real time if the number and size of the operators remain small.

8. Conclusion

This study concerned the construction of a parameterized reduced model of a hydroelastic problem with prestressing. In a recent paper [31], the prestress effects due to the geometrical nonlinearities induced by the weight of a liquid were calculated for different liquid heights, with a mapping of the structural part and a remeshing of the current liquid domain. A first originality of the present study was to map the liquid domain into an arbitrary reference domain that depends on the parameter. A second originality concerned the construction of reduced matrices in series form with separated variable operators obtained from an adapted SVD. An example based on an experiment from [32] demonstrated the feasibility and validity of the present method which takes into account the mutual influences of prestressing and added mass effect. How to interpolate the coefficients obtained via SVD for a larger number of parameters will be the subject of future developments, as well as the use of bases involving the contribution of added mass (improvement of what was done in [7] chapter 5 for different levels of liquid). Convergence analysis of the methodology for a larger number of hydroelastic modes and for

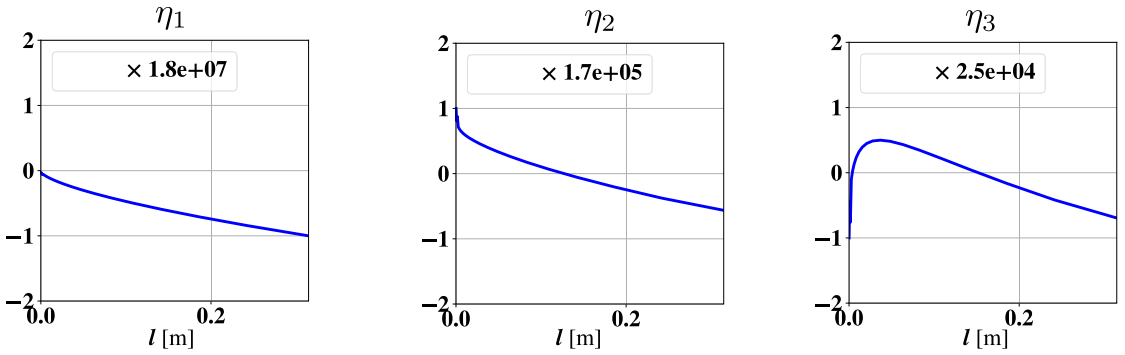

Fig. 13. Contributions of the reduced tangent stiffness matrices obtained via SVD as a function of the parameter l.

more complex numerical examples will be the next step of future investigations. This work could be used for the development of parameterized digital twins for the computation of various hydroelastic engineering problems, such as the hydroelastic behavior of liquid-propelled launch vehicles or future hybrid-hydrogen aircraft concepts, considering prestress effects due to the weight of the liquid.

Declaration of competing interest

The authors declare that they have no known competing financial interests or personal relationships that could have appeared to influence the work reported in this paper.

Data availability

No data was used for the research described in the article.

References

[1] H.N. Abramson, The Dynamic Behavior of Liquids in Moving Containers, with Applications to Space Vehicle Technology, NASA-SP-106, 1966, URL https://ntrs.nasa.gov/citations/19670006555.
[2] F.T. Dodge, The New "Dynamic Behavior of Liquids in Moving Containers", Southwest Research Inst., 2000.
[3] A.W. Leissa, Vibration of Shells, Scientific and Technical Information Office, National Aeronautics and Space Administration, 1973.
[4] M. Amabili, Effect of finite fluid depth on the hydroelastic vibrations of circular and annular plates, J. Sound Vib. 193 (4) (1996) 909–925, http://dx.doi.org/10.1006/jsvi.1996.0322.
[5] M.K. Kwak, S.B. Han, Effect of fluid depth on the hydroelastic vibration of free-edge circular plate, J. Sound Vib. 230 (1) (2000) 171–185, http://dx.doi.org/10.1006/jsvi.1999.2608.
[6] M. Amabili, A. Sarkar, M.P. Païdoussis, Reduced-order models for nonlinear vibrations of cylindrical shells via the proper orthogonal decomposition method, J. Fluids Struct. 18 (2) (2003) 227–250, http://dx.doi.org/10.1016/j.jfluidstructs.2003.06.002.
[7] H.J.-P. Morand, R. Ohayon, Fluid Structure Interaction, Wiley, 1995.
[8] J.T. Oden, J.N. Reddy, Variational Methods in Theoretical Mechanics, Springer Science & Business Media, 2012.
[9] T.E. Tezduyar, Y. Bazilevs, K. Takizawa, Computational Fluid-Structure Interaction: Methods and Applications, Wiley, 2013.
[10] T.M. van Opstal, E.H. van Brummelen, R. de Borst, M.R. Lewis, A finite-element/boundary-element method for large-displacement fluid-structure interaction, Comput. Mech. 50 (6) (2012) 779–788, http://dx.doi.org/10.1007/s00466-012-0794-7.
[11] W.C. Hurty, Dynamic analysis of structural systems using component modes, AIAA J. 3 (4) (1965) 678–685, http://dx.doi.org/10.2514/3.2947.
[12] R.R. Craig Jr., M.C.C. Bampton, Coupling of substructures for dynamic analyses, AIAA J. 6 (7) (1968) 1313–1317, http://dx.doi.org/10.2514/3.4741.
[13] U. Hetmaniuk, R. Tezaur, C. Farhat, Review and assessment of interpolatory model order reduction methods for frequency response structural dynamics and acoustics problems, Internat. J. Numer. Methods Engrg. 90 (13) (2012) 1636–1662, http://dx.doi.org/10.1002/nme.4271.
[14] G. Rozza, Reduced basis approximation and error bounds for potential flows in parametrized geometries, Commun. Comput. Phys. 9 (1) (2011) 1–48, http://dx.doi.org/10.4208/cicp.100310.260710a.
[15] R. Perez, X.Q. Wang, M.P. Mignolet, Nonintrusive structural dynamic reduced order modeling for large deformations: Enhancements for complex structures, J. Comput. Nonlinear Dynam. 9 (3) (2014) http://dx.doi.org/10.1115/1.4026155.
[16] J. Lighthill, Waves in Fluids, Cambridge University Press, 2001.

[17] J.S. Archer, C.P. Rubin, Improved Analytic Longitudinal Response Analysis For Axisymmetric Launch Vehicles. Volume I: Linear Analytic Model, Tech. Rep., NASA-CR-345, 1965, URL https://apps.dtic.mil/sti/citations/ADA455537.
[18] R. Coppolino, A Numerically Efficient Finite Element Hydroelastic Analysis, Tech. Rep., NASA-CR-2662, 1976, URL https://ntrs.nasa.gov/api/citations/19760016539/downloads/19760016539.pdf.
[19] A. Bermúdez, R. Rodríguez, D. Santamarina, A finite element solution of an added mass formulation for coupled fluid-solid vibrations, Numer. Math. 87 (2) (2000) 201–227, http://dx.doi.org/10.1007/s002110000175.
[20] E.H. van Brummelen, Added mass effects of compressible and incompressible flows in fluid-structure interaction, J. Appl. Mech. 76 (2) (2009) 021206, http://dx.doi.org/10.1115/1.3059565.
[21] R. Ohayon, C. Soize, Nonlinear model reduction for computational vibration analysis of structures with weak geometrical nonlinearity coupled with linear acoustic liquids in the presence of linear sloshing and capillarity, Comput. & Fluids 141 (2016) 82–89, http://dx.doi.org/10.1016/j.compfluid.2016.03.032.
[22] J.S. Mixson, R.W. Herr, An Investigation of the Vibration Characteristics of Pressurized Thin-Walled Circular Cylinders Partly Filled with Liquid, Tech. Rep., National Aeronautics and Space Administration, NASA-TR R-145, 1962.
[23] L. Pinson, C. Brown, A finite element method for nonaxisymmetric vibrations of pressurized shells of revolution partially filled with liquid, in: 14th Structures, Structural Dynamics, and Materials Conference, American Institute of Aeronautics and Astronautics, 1973, http://dx.doi.org/10.2514/6.1973-399.
[24] W.K. Liu, R.A. Uras, Transient failure analysis of liquid-filled shells part I: Theory, Nucl. Eng. Des. 117 (2) (1989) 107–140, http://dx.doi.org/10.1016/0029-5493(89)90037-X.
[25] J.-S. Schotté, R. Ohayon, Various modelling levels to represent internal liquid behaviour in the vibration analysis of complex structures, Comput. Methods Appl. Mech. Engrg. 198 (21) (2009) 1913–1925, http://dx.doi.org/10.1016/j.cma.2008.12.016.
[26] J.-S. Schotté, R. Ohayon, Linearized formulation for fluid–structure interaction: Application to the linear dynamic response of a pressurized elastic structure containing a fluid with a free surface, J. Sound Vib. 332 (10) (2013) 2396–2414, http://dx.doi.org/10.1016/j.jsv.2012.07.036.
[27] M. Haßler, K. Schweizerhof, On the static interaction of fluid and gas loaded multi-chamber systems in large deformation finite element analysis, Comput. Methods Appl. Mech. Engrg. 197 (19–20) (2008) 1725–1749, http://dx.doi.org/10.1016/j.cma.2007.08.028.
[28] C. Hoareau, J.F. Deü, Nonlinear equilibrium of partially liquid-filled tanks: A finite element/level-set method to handle hydrostatic follower forces, Int. J. Non-Linear Mech. 113 (2019) 112–127, http://dx.doi.org/10.1016/j.ijnonlinmec.2019.03.014.
[29] H.D. Hibbit, Some follower forces and load stiffness, Internat. J. Numer. Methods Engrg. 14 (6) (1979) 937–941, http://dx.doi.org/10.1002/nme.1620140613.
[30] P. Podio-Guidugli, A variational approach to live loadings in finite elasticity, J. Elasticity 19 (1) (1988) 25–36, http://dx.doi.org/10.1007/BF00041693.
[31] C. Hoareau, J.F. Deü, R. Ohayon, Hydroelastic linearized vibrations taking into account prestressed effects due to internal liquid weight: numerical vs. experimental results, J. Fluids Struct. 112 (2022) 103596, http://dx.doi.org/10.1016/j.jfluidstructs.2022.103596.
[32] M. Chiba, Nonlinear hydroelastic vibration of a cylindrical tank with an elastic bottom, containing liquid. Part I: Experiment, J. Fluids Struct. 6 (2) (1992) 181–206, http://dx.doi.org/10.1016/0889-9746(92)90044-4.
[33] M. Chiba, Nonlinear hydroelastic vibration of a cylindrical tank with an elastic bottom, containing liquid. Part II: Linear axisymmetric vibration analysis, J. Fluids Struct. 7 (1) (1993) 57–73, http://dx.doi.org/10.1006/jfls.1993.1005.
[34] P.G. Ciarlet, Three-Dimensional Elasticity, Elsevier, 1988.
[35] J. Bonet, R.D. Wood, Nonlinear Continuum Mechanics for Finite Element Analysis, Cambridge University Press, 2008.
[36] T. Wick, Fluid-structure interactions using different mesh motion techniques, Comput. Struct. 89 (13–14) (2011) 1456–1467, http://dx.doi.org/10.1016/j.compstruc.2011.02.019.
[37] Q. Akkaoui, E. Capiez-Lernout, C. Soize, R. Ohayon, Solving generalized eigenvalue problems for large scale fluid-structure computational models with mid-power computers, Comput. Struct. 205 (2018) 45–54, http://dx.doi.org/10.1016/j.compstruc.2018.04.007.
[38] G.H. Golub, C.F.V. Loan, Matrix Computations, fourth ed., Johns Hopkins University Press, Baltimore, 2013.